Am J Cancer Res 2022;12(4):1465-1483
www.ajcr.us /ISSN:2156-6976/ajcr0141086

Original Article

DNA repair proteins as the targets for paroxetine to induce cytotoxicity in gastric cancer cell AGS

Bang-Hung Liu[1], Tein-Ming Yuan[2], Chih-Jou Huang[1], Duan-Ting Hsu[1], Shi-Wen Chen[2], Nai-Wan Hsiao[3], Sheng-Chih Lin[1], Shu-Wan Wu[4,5], Yi-Mei J Lin[1], Show-Mei Chuang[1]

[1]Institute of Biomedical Sciences, National Chung Hsing University, Taichung 402, Taiwan; [2]Department of Surgery, Feng Yuan Hospital, Ministry of Health and Welfare, Taichung 420, Taiwan; [3]Department of Biology, National Changhua University of Education, Changhua 500, Taiwan; [4]Institute of Molecular Biology, Academia Sinica, Taipei 115, Taiwan; [5]College of Life Sciences, Inservice Master Program in Life Sciences, National Chung Hsing University, Taichung 402, Taiwan

Received December 13, 2021; Accepted March 16, 2022; Epub April 15, 2022; Published April 30, 2022

Abstract: To evaluate the potential anticancer effects of 1175 FDA-approved drugs, cell viability screening was performed using 25 human cancer cell lines covering 14 human cancer types. Here, we focus on the action of paroxetine, which demonstrated greater toxicity toward human gastric adenocarcinoma cell-line AGS cells compared with the other FDA-approved drugs, exhibiting an IC50 value lower than 10 μM. Evaluation of the underlying novel mechanisms revealed that paroxetine can enhance DNA damage in gastric cancer cells and involves downregulation of Rad51, HR23B and ERCC1 expression and function, as well as nucleotide shortage. Enhancement of autophagy counteracted paroxetine-induced apoptosis but did not affect paroxetine-induced DNA damage. Paroxetine also enhanced ROS generation in AGS cells, but a ROS scavenger did not improve paroxetine-mediated DNA damage, apoptosis, or autophagy, suggesting ROS might play a minor role in paroxetine-induced cell toxicity. In contrast, paroxetine did not enhance DNA damage, apoptosis, or autophagy in another insensitive gastric adenocarcinoma cell-line MKN-45 cells. Interestingly, co-administration of paroxetine with conventional anticancer agents sensitized MKN-45 cells to these agents: co-treated cells showed increased apoptosis relative to MKN-45 cells treated with the anticancer agent alone. Unequivocally, these data suggest that for the first time that paroxetine triggers cytotoxicity and DNA damage in AGS cells at least partly by reducing the gene expression of Rad51, HR23B, and ERCC1. Our findings also suggest that paroxetine is a promising candidate anticancer agent and/or chemosensitizing agent for use in combination with other anticancer drugs in cancer therapy. The molecular mechanisms underlying the anticancer activity of co-treatment with paroxetine and chemotherapy appear to be complex and are worthy of further investigation.

Keywords: Gastric cancer, paroxetine, apoptosis, DNA damage, drug repurposing, chemosensitizer

Introduction

Chemotherapy is a promising treatment for human tumors, but its scope of efficacy is restricted. Application of chemotherapeutic agents is often hindered from toxicity and the emergence of intrinsic resistance after long-term employment. Therefore, it is important to develop new chemicals that are effective against specific cancers with different genotypic backgrounds. In addition, more effective and safer treatment strategies that combine a low dosage of chemotherapeutic agents with other agents might decrease anticancer drug-related side effects and chemoresistance. For instance, combination of chemotherapeutic drugs and natural compounds has been reported to ameliorate the efficacy of anticancer therapy [1-4].

Drug repositioning, the search for new therapeutic indications of drugs approved for other diseases, has received considerable attention recently. With a wealth of clinical data on how drugs work in the body and their potential toxicity, drug repositioning could be a very effective alternative for the development of anticancer drugs compared to traditional time-consuming

and expensive cancer drug development programs. Selective serotonin reuptake inhibitors (SSRIs) are among the most commonly used antidepressants, due to their effectiveness, superior safety profile, and tolerability. SSRIs, including fluoxetine, sertraline, and paroxetine, have been the subject of intense study in recent years because they have been found to inhibit cell proliferation and evoke cell death via apoptosis in various human cancer cell lines, including those derived from lymphoma, colon cancer, osteosarcoma, and hepatocellular carcinoma [5-9].

Paroxetine is a potent and selective FDA-approved SSRI that shows antidepressant activity believed to be related to this activity. Outside the original scope of antidepressants, the anticancer effects of paroxetine have been recently identified in various types of cancer cells. Epidemiologic research on the use of paroxetine in cancer patients has indicated that its use is associated with decreased risks of colorectal cancer [10] and epithelial ovarian cancer [11], whereas its effect on breast cancer outcome is controversial [12, 13]. Paroxetine has been reported to modulate multiple processes involving different cellular functions, leading to anticancer effects. It has been shown to inhibit DNA synthesis in biopsy-like Burkitt lymphoma cells [9], reduce cell viability and induce apoptosis in various cancer cells, including rat C6 glioma cells, human SH-SY5Y neuroblastoma cells, MG63 osteosarcoma cells, human HT29, LS1034 colon adenocarcinoma cells and human HepG2 hepatocellular carcinoma cells [5-7, 14]. Similar anticancer effects were also identified in HT29-xenografted mice [6]. Mechanistic studies have shown that paroxetine can influence several signaling pathways involved in tumor progression (e.g., the MET, ERBB3, p38, and JNK pathways) depending on the genetic background [5, 15-17]. Paroxetine has been reported to associate with cytochrome P450 (CYP450) enzymes (such as CYP2D6) [18], G protein-coupled receptor kinase 2 (GRK2) [19], and phosphofructokinase (PFK) [20]. Interestingly, an in silico-in vitro fishing strategy and kinase assay demonstrated that paroxetine effectively inhibits c-Src family kinase members (e.g., ABL, SRC, KIT, MET, and FYN) in vitro [21].

We have performed a large-scale screen of FDA-approved drugs against multiple human cancer cell lines and found that paroxetine demonstrated the greatest toxicity toward gastric adenocarcinoma AGS cells (**Figure 1**). Although apoptosis and signaling pathways are known to be functionally involved in cancers, they do not fully explain the sophisticated cytotoxic effects of paroxetine on cancer cells. Moreover, little research has examined the genotoxic capacity of paroxetine. This study was designed to investigate the molecular mechanisms through which paroxetine interacts with the components of signaling machineries and provide new insight into its anticancer effects. We successfully revealed a novel mechanism whereby paroxetine inhibits AGS cell proliferation in the micromolar range by inhibiting the expression of DNA repair proteins and increasing DNA damage, leading to the activation of apoptotic cell death. In addition, the combinatorial effect of paroxetine and oncology drugs was investigated. We report for the first time that the expression levels of Rad51, HR23B, and ERCC1 are severely impaired by paroxetine, probably via downregulation of POU3F2 protein, leading to higher cytotoxicity and unrepaired DNA damage in AGS cells compared to MKN-45 cells.

Materials and methods

Chemicals and antibodies

The FDA-approved drug library and paroxetine were purchased from Selleckchem (Houston, Texas, USA). Chloroquine (CQ), N-acetyl-cysteine (NAC), 5-fluorouracil (5-FU), cisplatin, docetaxel, and doxorubicin were obtained from Sigma-Aldrich (St. Louis, MO, USA). Specific monoclonal antibodies against β-actin, Rad51, AKT, ERK1/2, p38, JNK, Chk1, and P-glycoprotein were obtained from Santa Cruz Biotechnology (Dallas, TX, USA). Polyclonal antibodies against poly(ADP-ribose) polymerase (PARP), phospho-AKT (Ser473), phospho-ERK1/2 (Thr-202/Tyr204), phospho-p38 (Thr180/Tyr182), phospho-JNK (Thr183/Tyr185), phospho-Chk1 (Ser345), γ-H2AX, Bax, caspase 3, ATG5, LC3B, and POU3F2 were obtained from Cell Signaling Technology (Beverly, MA, USA). ERCC1 was obtained from ABclonal (Woburn, MA, USA). The antibody against HR23B was purchased from Millipore (Bedford, MA, USA), and that against HR23A was obtained from Abnova (Taipei, Taiwan).

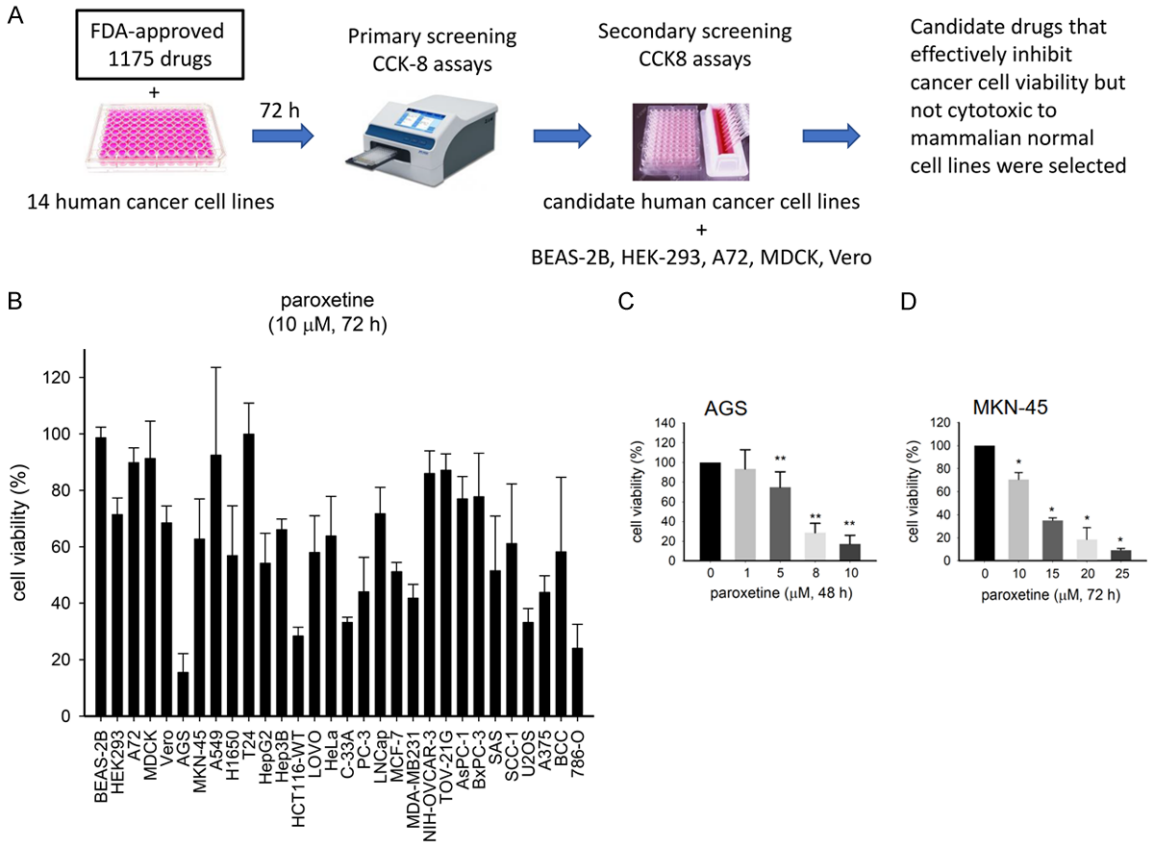

Figure 1. The flow diagram of drug screening and validation for potential anti-cancer drugs. (A, B) 14 human cancer cell lines were treated with 10 μM FDA-approved 1175 drugs for 72 hours. The cell viability was determined by CCK-8. All experiments were performed in triplicate and in four batches. Cell viability of each cell line under paroxetine treatment is expressed as a percentage compared to 0.1% DMSO-treated control. (C) AGS and (D) MKN-45 were treated with different doses of paroxetine for 48 hours and 72 hours, respectively, and the cell viability and IC50 were determined by CCK-8. Data are representative of four to five independent experiments.

Cell culture

Human gastric adenocarcinoma cell lines AGS and MKN-45 cells were cultured in RPMI medium (Invitrogen) supplemented with 10% fetal bovine serum (FBS; Invitrogen, Carlsbad, CA, USA) and penicillin/streptomycin (Invitrogen), at 37°C in a humidified incubator containing 5% CO_2 in air. AGS was provided by Dr. Chun-Ying Wu (Taipei Veterans General Hospital, Taipei, Taiwan) [22, 23]. MKN-45 was purchased from the Japanese Collection of Research Bioresources Cell Bank (Osaka, Japan).

Cell counting kit-8 (CCK-8) assay

Cell viability was quantitated using a CCK-8 assay (Dojindo Molecular Technologies, Kumamoto, Japan). Briefly, cells (5×10^3/well) were seeded into 96-well plates and incubated overnight before treatment with paroxetine or paroxetine plus a conventional anticancer drug. After 48 hours or 72 hours, addition of 10 μl CCK-8 reagent to each well as recommended by the manufacturer. Finally, spectrophotometric absorbance was measured with a microplate reader (Multiskan FC; Thermo Fisher Scientific, Vantaa, Finland) at 450 nm. The data are given as the means ± SD of four to five independent experiments and each experiment was performed in triplicate.

Western blot analysis

Cell extracts were harvested with lysis buffer consisting of 20 mM Tris-HCl (pH 7.4), 100 mM NaCl, 5 mM EDTA, and a protease inhibitor cocktail (Roche, Germany). Equal amounts of protein were subjected to sodium dodecyl sulfate polyacrylamide gel electrophoresis (SDS-

PAGE) and transferred to PVDF membranes (Millipore). Membranes were blocked, washed, and probed with primary antibodies, then each primary antibody was removed by washing and then incubated with the appropriate horseradish peroxidase-conjugated secondary antibodies (Jackson Immuno Research Laboratories, West Grove, PA, USA) for 1 hour. The target proteins were then detected using enhanced chemiluminescence (ECL) reagents, according to the manufacturer's instructions (Millipore). Each experiment was performed independently at least four times.

Quantitative real-time PCR (qRT-PCR)

TRIzol reagent (Invitrogen) was used to extract total RNA from cells under specific conditions. Specific primers for quantitative real-time PCR were designed using the Probe Finder software from Roche Applied Science (available online at the Universal ProbeLibrary Assay Design Center) based on the MIQE (Minimum Information for Publication of Quantitative Real-Time PCR Experiments) Guidelines. Quantitative real-time PCR analysis was performed with a LightCycler Nano instrument (Roche). Each sample was analyzed three times in triplicate. HPRT (hypoxanthine phosphoribosyltransferase) was used as the internal control. Fold changes of mRNA expression in different cells were determined by $2^{-\Delta\Delta CT}$ method.

Flow cytometry

Cells cultured in 6-cm dishes were enzymatically digested with 0.25% trypsin-EDTA and collected by centrifugation followed by fixing with 70% ethanol for 2 hours. The fixed cells were then stained with 50 μg/ml propidium iodide (PI; Sigma-Aldrich) and 200 μg/ml RNaseA (Sigma-Aldrich) in PBS for 30 min, and the cell cycle distribution was analyzed using Beckman Coulter FC500 flow cytometer (Beckman Coulter Inc., Brea, CA, USA). Intracellular ROS generation was evaluated by dichlorodihydrofluorescein diacetate assay (H2DCFDA; Calbiochem, San Diego, CA, USA). Cells were harvested, washed with PBS, and incubated with 5 μM H2DCFDA at 37°C for 30 min in the dark. The cells were then washed three times with PBS, resuspended in PBS, and subjected to flow cytometric analysis of cellular fluorescence signals. The images shown are representative of at least five independent experiments carried out under the same conditions.

Measurement of cellular accumulation of rhodamine 123

The measurement of cellular accumulation of rhodamine 123 (Sigma-Aldrich), a fluorescent substrate of P-glycoprotein, was performed by a flow cytometer (Beckman Coulter) equipped with an ultraviolet argon laser (excitation at 488 nm and emission at 530 ± 15 nm), as described previously [24]. Cells were incubated with 0.1 μM rhodamine 123 in the absence or presence of 10 μM paroxetine for 30 min at 37°C. The cells were then washed with ice-cold PBS and trypsinized, and the fluorescence intensity of rhodamine 123 in individual cells was measured immediately by a flow cytometer. The data shown are representative of at least three independent experiments carried out under the same conditions.

Cell division

Cells were labeled with 5 μM Cell Tracker Green (5-chloromethylfluorescein diacetate [CMFDA]; Molecular Probes, Eugene, OR, USA) for 30 min at 37°C, washed with PBS, and given fresh medium supplied with 10 μM paroxetine. After 48 hours, the cells were trypsinized, washed twice with PBS, suspended in PBS, and subjected to flow cytometry to detect cellular fluorescence signals. The images shown are representative of at least three independent experiments carried out under the same conditions.

Mitochondrial membrane potential (MMP)

Changes in MMP were detected by staining cells with the fluorescent probe, JC-10 (AAT Bioquest, Sunnyvale, CA, USA). Briefly, cells (5×10^5/60-mm dish) were treated with or without paroxetine for 24 hours, harvested, and stained with 10 μM JC-10 reagent at 37°C for 15 min. The cell fluorescence was immediately analyzed using a flow cytometer. The images shown are representative of at least four independent experiments carried out under the same conditions.

Immunofluorescence staining

Cells grown on cover slides were washed with PBS, fixed in 4% formaldehyde/PBS, washed in PBS, and blocked in 5% bovine serum albumin/PBS. Cells were incubated with primary antibodies (in 5% bovine serum albumin/PBS) overnight at 4°C, followed by washing. Primary anti-

body binding was detected with rhodamine-conjugated goat anti-rabbit (Millipore). Fluorescence images were collected on an Olympus IX71 fluorescence microscope (Olympus, Tokyo, Japan). The data shown were carried out with at least three independent experiments under the same conditions.

Evaluation of DNA repair ability by GFP reporter

For cisplatin-damaged DNA, pEGFP plasmids were incubated with 1 μg/ml cisplatin at 37°C for 2 hours. The cisplatin-treated plasmids were purified and transfected into cells. After 12-hour transfection, cells were treated with 10 μM paroxetine for another 6-24 hours. The untreated pEGFP plasmid was as the control. The GFP fluorescence was detected at indicated time periods by Olympus IX71 fluorescence microscope [25].

Combined drug analysis

The combined effect of paroxetine and various oncology drugs on MKN-45 cells was assessed using the CompuSyn software (ComboSyn, Inc., Paramus, NJ, USA). The combined effects of paroxetine and various anticancer drugs on MKN-45 cells were evaluated using CompuSyn software (ComboSyn, Inc., Paramus, NJ, USA), which evaluates the drug interactions based on the combination index (CI)-isobologram equation method [26, 27]. The combined effect was classified as follows: CI < 1 implied synergism, CI = 1 implied additivity, and CI > 1 implied antagonism.

Statistical analysis

For statistical analysis, each experimental value was compared to its corresponding control. The statistical significance of differences between mean values was estimated using the t-test. *P*-values less than 0.05 were considered statistically significant. Data are presented as the mean ± SD of the indicated number of biological replicates.

Results

Paroxetine significantly inhibits the cell viability of AGS cells

The development of novel pharmacological approaches and targets has become a high priority in chemotherapy. Drug repurposing is a promising option, as repurposed drugs may act as anticancer therapeutics. To assess the antitumor effects of a large group of FDA-approved non-anticancer drugs, 25 cancer cell lines representing 14 types of human cancer were preliminarily exposed to 10 μM of various FDA-approved drugs for 72 hours, and cell viability was screened by CCK-8 assay (**Figure 1A** and **1B**). The candidates that effectively inhibited the cell viability of specific cancer cell lines were further assessed. Among them, the effect of paroxetine on the viability of AGS cells was of particular interest, as paroxetine demonstrated the greatest toxicity toward AGS cells and it is a commonly used antidepressant due to its effectiveness, superior safety profile, and tolerability. We found that paroxetine inhibited the cell viability of AGS cells far more robustly than the other 24 cancer cell lines tested herein (**Figure 1B**). AGS cells exhibited a marked dose-dependent decrease of viability in response to a 48-h exposure to paroxetine (survival rate = 14.14%, IC50 = 6.2 μM at 48 hours; **Figure 1C**). The IC50 of paroxetine in AGS cells was lower than that in MKN-45 cells (IC50 = 11.9 μM at 72 hours). MKN-45 cells were relatively resistant to the action of paroxetine; there was little change in viability at a dose of 5 μM, and even at 10 μM the survival rate remained as high as 73% after 72 hours (**Figure 1D**).

Flow cytometry revealed a remarkable increase in the sub-G1 population of AGS cells exposed to paroxetine, indicating that this treatment enhanced apoptosis in dose- and time-dependent manners (**Figure 2A-C**). Consistently, we observed increases in the levels of active caspase 3, cleaved PARP, and Bax (**Figure 2D**) in paroxetine-treated AGS cells, indicating that the paroxetine-induced inhibition of AGS cell viability was mediated through the induction of caspase 3-dependent apoptosis. Analysis of apoptotic markers showed that paroxetine did not trigger significant cytotoxicity in MKN-45 cells (**Figure 2D**). Further analysis of signaling pathways indicated that the level of phospho-AKT gradually decreased, whereas phospho-JNK gradually increased in paroxetine-treated AGS (**Figure 2E**). This suggests that the cell viability decrease seen in paroxetine-treated AGS cells might be due to upregulation of apoptotic proteins on the one hand and downregulation of survival-related proteins on the other. A CMFDA accumulation assay confirmed that cell

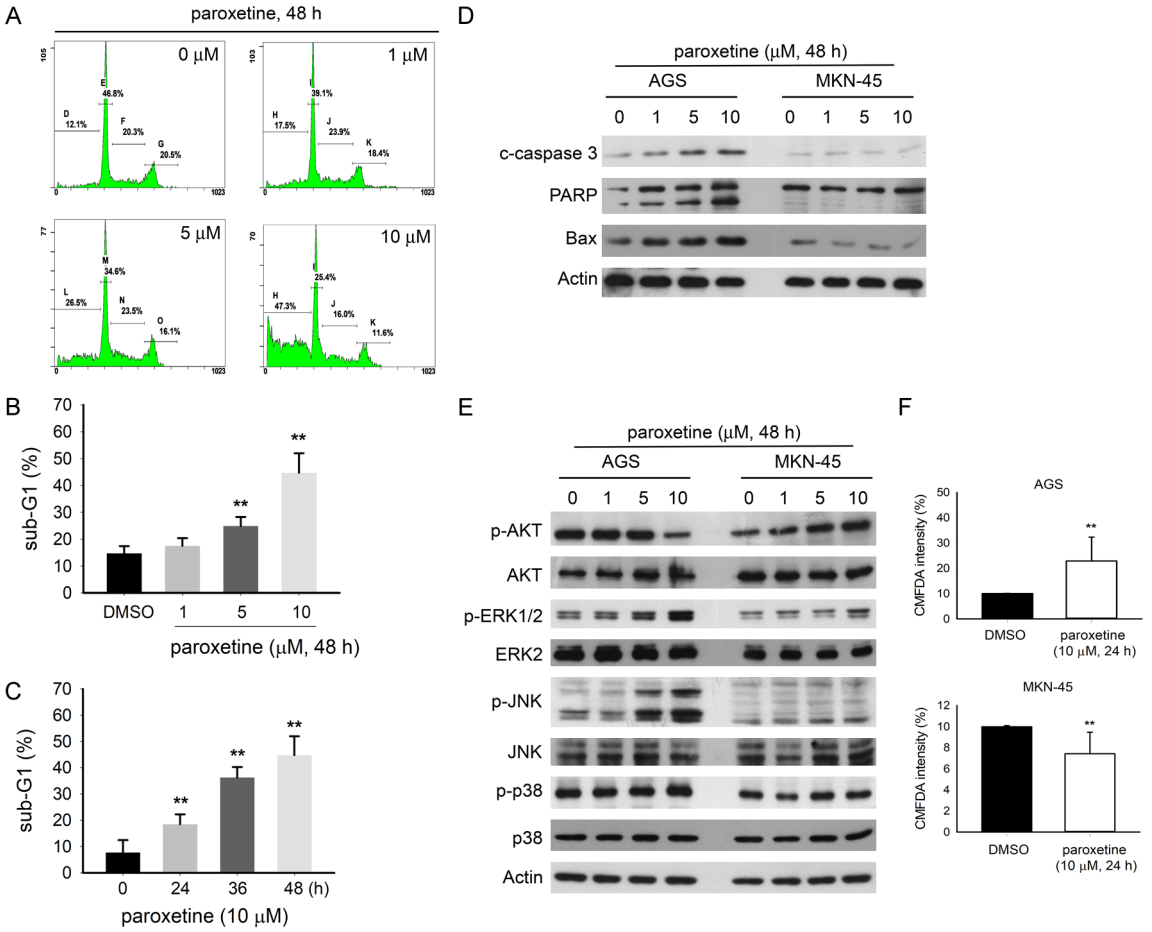

Figure 2. The induction of apoptosis by paroxetine in AGS. A-C. After 48-hour treatment, the levels of sub-G1 in AGS were determined by flow cytometry analysis. D. The apoptotic markers, cleaved PARP, active caspase 3, and Bax were measured by Western blot assays following the treatment of paroxetine. E. The Western blot analysis was performed to assay the activation of AKT, ERK, JNK, and p38 signaling in AGS and MKN-45 with different doses of paroxetine treatment for 48 hours. F. The cell division rate was determined by CMFDA staining followed by flow cytometry analysis after 24-hour treatment of paroxetine. Data are representative of four to six independent experiments.

division was attenuated following paroxetine treatment in AGS cells, but not in MKN-45 cells (**Figure 2F**), further suggesting that paroxetine does not greatly affect the growth of MKN-45 cells.

Paroxetine induces DNA damage by downregulating DNA damage repair proteins in AGS cells

Although the anticancer ability of paroxetine has been reported, the detailed mechanisms underlying such effects are unknown. Here, we sought to investigate the mechanism underlying the high sensitivity of AGS cells to paroxetine. We found that paroxetine treatment for 48 hours increased DNA damage in AGS cells but not MKN-45 cells: In AGS cells, paroxetine enhanced the levels of Ser139-phosphorylated subtype H2AX (γ-H2AX), which is an indicator of damaged DNA with strand breaks (**Figure 3A**), as well as the levels of p53 and phospho-Chk1, which further signal an increase of DNA damage-mediated cell cytotoxicity. Further assessments revealed that some DNA damage repair proteins were significantly decreased by paroxetine. More specifically, the protein levels of Rad51, HR23B (but not HR23A, data not shown), and ERCC1 were dose- and time-dependently lowered by paroxetine in AGS cells, but not MKN-45 cells (**Figure 3A** and **3B**). Immunofluorescence staining confirmed that the levels of γ-H2AX foci were increased in the nuclei of paroxetine-treated AGS cells (**Figure 3C**). Consistent with the results presented in **Figure 2E**, the time-dependent increase in apoptosis among paroxetine-treated AGS cells

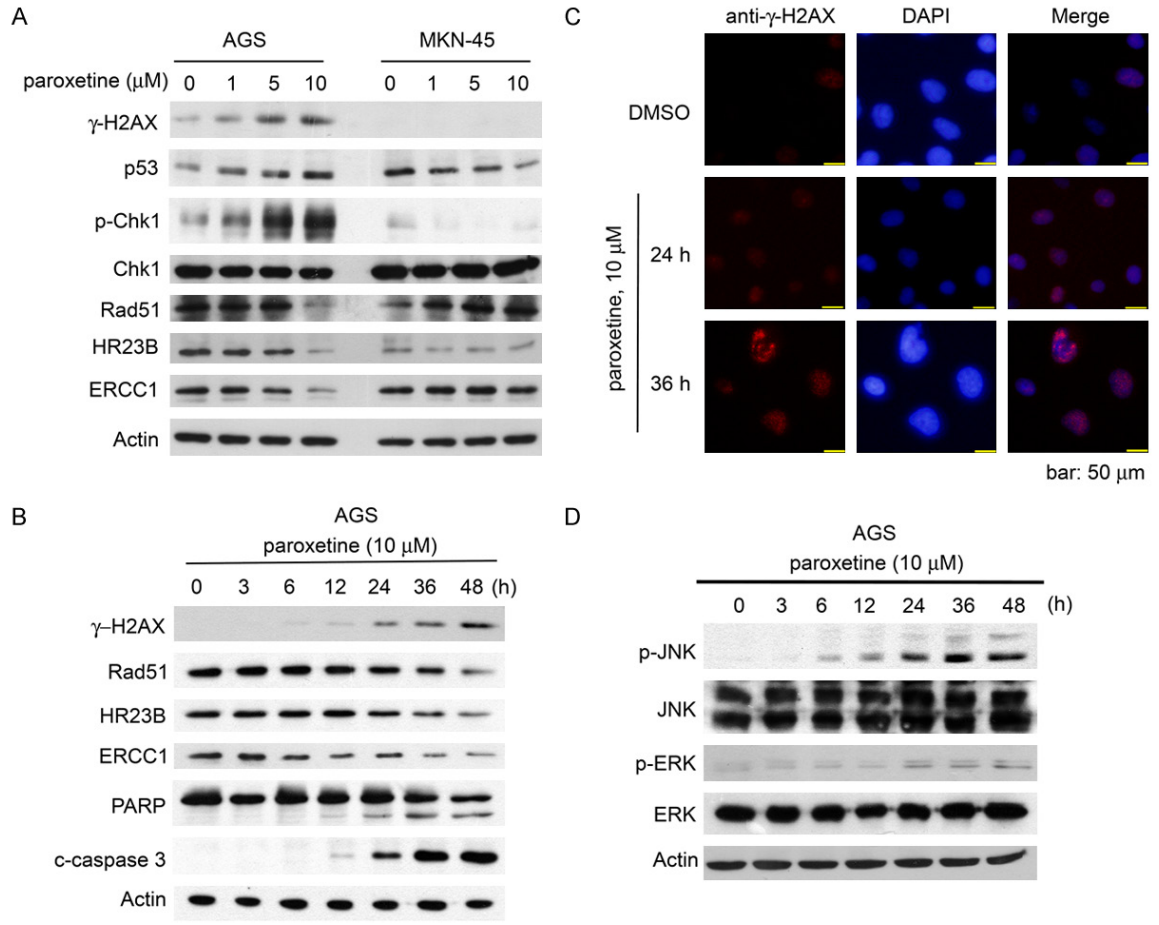

Figure 3. Paroxetine induces DNA damage in AGS. A. Expression of DNA damage markers and DNA repair proteins in cells treated with different doses of paroxetine for 48 hours were detected by immunoblotting assays. B. AGS was exposed to 10 μM paroxetine and the protein levels of DNA repair proteins and apoptosis markers were measured at indicated time points. C. After 10 μM paroxetine treatment for 24 and 36 hours, the expression of γ-H2AX in AGS cells was detected by immunofluorescence staining, and DMSO treatment was used as a control. Scale bar = 50 μm. D. AGS was exposed to 10 μM paroxetine and the protein levels of phospho-JNK and phospho-ERK were measured at indicated time points. Data are representative of three to five independent experiments.

corresponded to increases in phospho-JNK and phospho-ERK (**Figure 3D**).

Quantitative RT-PCR assays revealed that paroxetine significantly suppressed the mRNA expression levels of Rad51, HR23B, and ERCC1 in AGS cells (**Figure 4A**), indicating that paroxetine downregulated Rad51, HR23B, and ERCC1 at the transcriptional level. Moreover, we found that recovering the expression levels of HR23B and Rad51 partially reversed paroxetine-induced DNA damage and apoptosis (**Figure 4B**). Due to the down-regulation of Rad51, HR23B and ERCC1 expression, we speculated that paroxetine reduced the efficiency of DNA damage repair. To confirm the effect of paroxetine on DNA repair function, pEGFP plasmid was treated with cisplatin in vitro and then transfected into cells for repair. The restoration of GFP fluorescence can be used as an indicator of the efficacy of DNA repair, because unrepaired DNA damage temporarily represses gene transcription. **Figure 4C** showed that the fluorescence of untreated pEGFP increased with time regardless of paroxetine treatment for 6-24 hours (**Figure 4C**, the first and second panels). In contrast, the fluorescence recovery of cisplatin-treated pEGFP was significantly delayed compared to untreated pEGFP (**Figure 4C**, the third group); and paroxetine treatment further delayed the fluorescence recovery of cisplatin-treated pEGFP (**Fig-**

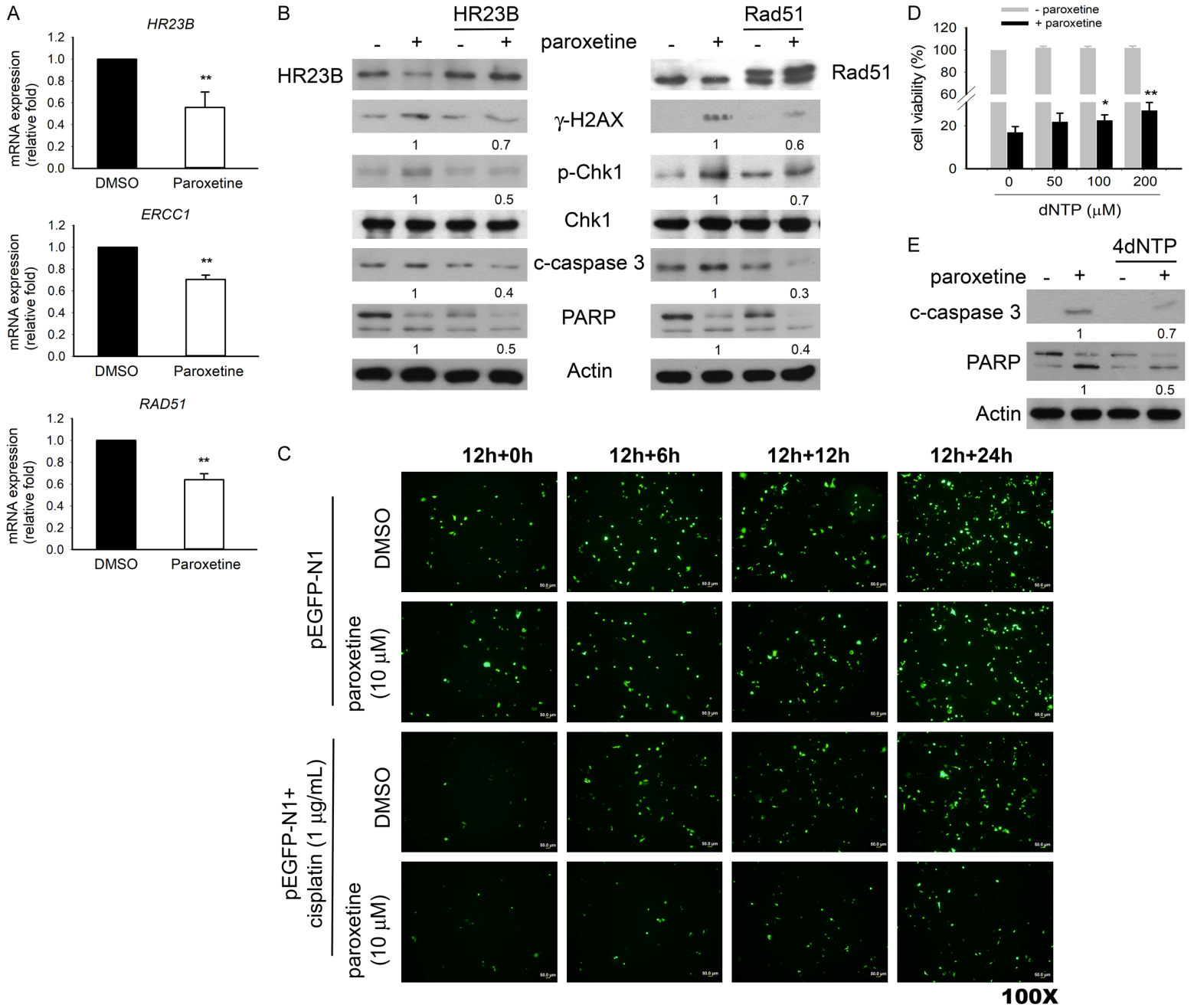
A
HR23B
ERCC1
RAD51
mRNA expression (relative fold)
DMSO
Paroxetine
B
HR23B
Rad51
paroxetine
γ-H2AX
p-Chk1
Chk1
c-caspase 3
PARP
Actin
D
- paroxetine
+ paroxetine
cell viability (%)
dNTP (μM)
E
4dNTP
paroxetine
c-caspase 3
PARP
Actin
C
12h+0h
12h+6h
12h+12h
12h+24h
pEGFP-N1
DMSO
paroxetine (10 μM)
pEGFP-N1+ cisplatin (1 μg/mL)
100X

Figure 4. Rad51, HR23B, and ERCC1 gene expression were down-regulated by paroxetine. A. AGS was exposed to 10 μM paroxetine for 24 hours and the mRNA levels of Rad51, HR23B, and ERCC1 were measured by qRT-PCR. B. HR23B and Rad51 were overexpressed in AGS for 24 hours followed by treatment of paroxetine for 48 hours, and the levels of DNA damage markers and apoptotic proteins were determined by Western blot assays. C. pEGFP plasmids were incubated with 1 μg/ml cisplatin at 37 °C for 2 hours. The cisplatin-treated plasmids were purified and transfected into AGS cells. After 12-hour transfection, cells were treated with 10 μM paroxetine for 6, 12, or 24 hours. The untreated pEGFP plasmid was as the control. D. AGS was treated with different concentrations of 4dNTP in the presence or absence of 10 μM paroxetine for 48 hours before measurement of cell viability. E. AGS was treated with 10 μM paroxetine in the presence or absence of 200 μM 4dNTP for 48 hours, and the cleaved caspase 3 (c-caspase 3) and PARP were measured by Western blot assays. Data are representative of three to five independent experiments.

ure 4C, the fourth panel). These results indicated that paroxetine might target genes related to DNA repair to suppress DNA repair ability and elicit cytotoxicity. In addition, an insufficient supply of nucleotides during DNA replication is associated with slow replication fork progression (resulting in DNA damage and genomic instability) and DNA repair deficiency. If DNA damage is not repaired, cells may initiate apoptotic responses [28, 29]. Therefore, we tested whether an additional supply of nucleotides could reverse the paroxetine-induced cell viability loss and apoptosis of AGS cells. Indeed, addition of the four deoxynucleotides slightly rescued the decreased cell viability (**Figure 4D**) and increased apoptosis (**Figure 4E**) seen in paroxetine-treated AGS cells. Since damage to the genetic material is a significant inducer of further apoptosis, we suggest that paroxetine-induced deficiencies in DNA repair ability and insufficiencies in nucleosides/nucleotides might cause severe DNA damage that goes unrepaired, leading to decreased cell survival. The observed differences in the effect of paroxetine on AGS versus MKN-45 cells was not due to a difference in the drug excretion system, as the protein level and excretion activity of P-glycoprotein were not different between the two cell lines (Supplemental Figure 1A and 1B). Furthermore, we also investigated the metabolites of paroxetine [30] and found no significant difference in the paroxetine-metabolizing activity of AGS and MKN-45 cells (Supplemental Figure 1C). These results suggest that paroxetine might directly modulate cell biological processes, such as gene transcription and/or nucleoside/nucleotide metabolism, and further indicate that the anticancer apoptosis-inducing effect of paroxetine in AGS cells might involve DNA damage responses other than those of the serotonergic system.

Autophagy is dispensable for the DNA damage response induced by paroxetine

We further demonstrated that paroxetine dose-dependently enhanced autophagy in AGS cells (**Figure 5A-C**). Autophagy is an evolutionarily conserved cellular process that plays central roles in maintaining cellular homeostasis and physiology. The role of autophagy in cancer is controversial, and appears to depend on the cancer type, genetic context, and/or disease stage. To confirm the role of paroxetine in inducing autophagy in AGS cells, we performed experiments involving chloroquine, which prevents the autophagosome from fusing with the lysosome. We found that chloroquine further enhanced the paroxetine-induced protein levels of LC3-II and p62, which are widely used to monitor autophagy. Chloroquine also increased the paroxetine-induced levels of cleaved PARP and active caspase 3 (**Figure 5D**), implying that autophagy might be used to eliminate the harmful organelles and maintain cellular physiology. Chloroquine co-treatment did not affect the level of DNA damage or the downregulations of HR23B and Rad51 proteins (**Figure 5E**) or JNK signaling (**Figure 5F**) in paroxetine-treated AGS cells. Together, these results imply that autophagy induction might counteract paroxetine-mediated apoptosis in AGS cells, but that autophagy is suggested to no obvious effect on paroxetine-induced DNA damage responses. However, we cannot exclude the possibility that autophagy might play a compensatory role in paroxetine-induced DNA damage responses.

ROS is dispensable for the DNA damage induced by paroxetine

ROS is one of the most important mediators of DNA damage and apoptosis. Medication-induced elevation of ROS can be used to target

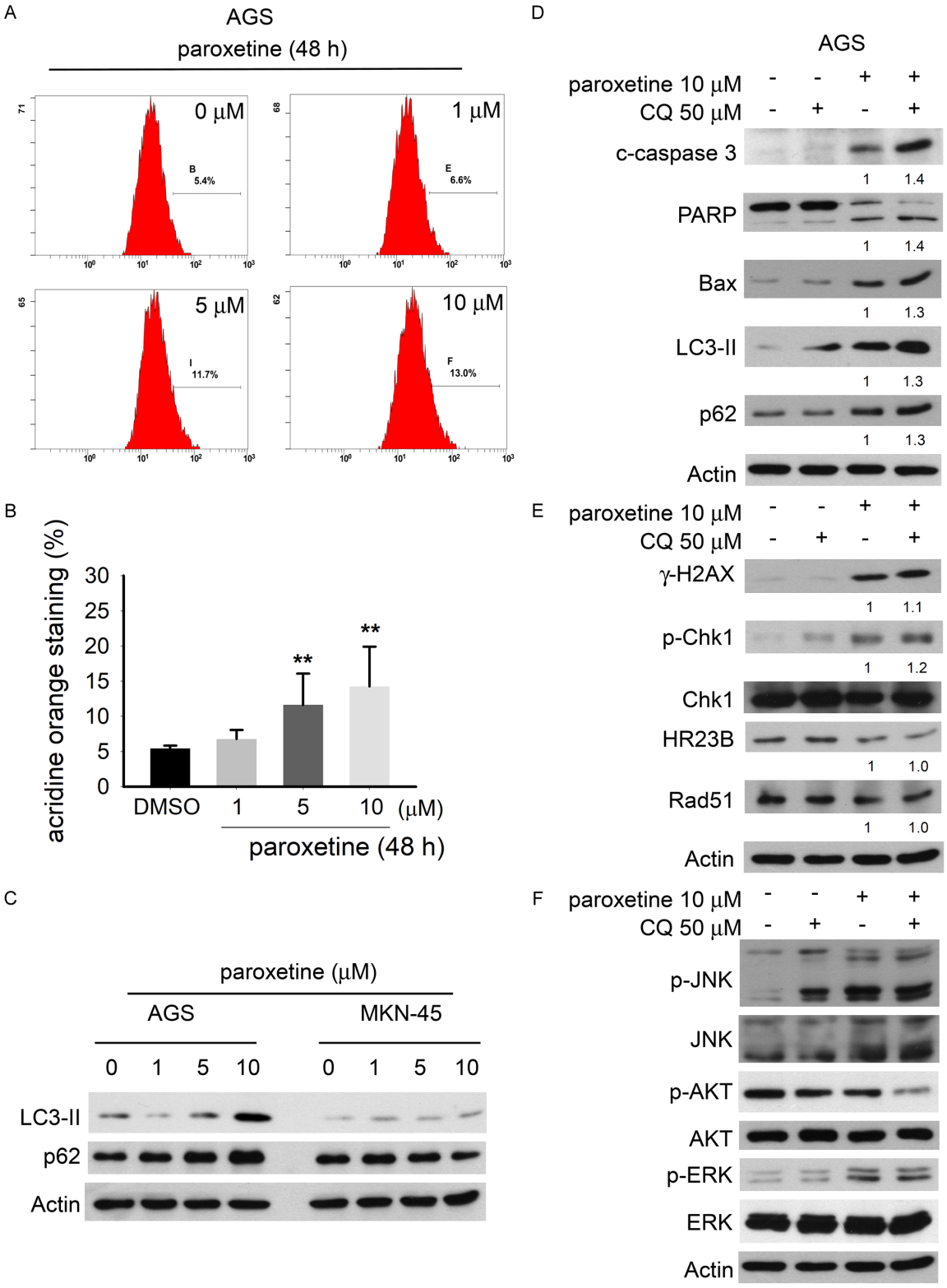

Figure 5. Autophagy counteracts paroxetine-induced apoptosis in AGS. (A, B) AGS cells were treated with 10 μM paroxetine for 48 hours, and then stained with acridine orange to determine the levels of autolysosomes by flow cytometry. (C) Cells were exposed to different doses of paroxetine for 48 hours, and then the levels of autophagy markers were determined by Western blot assays. AGS cells were treated with paroxetine for 42 hours and then co-treated with chloroquine (CQ) for another 6 hours. The levels of apoptosis and autophagy markers (D), DNA damage markers and DNA repair proteins (E) and signaling (F) were determined by Western blot assays. All experiments were performed in four to seven replicates.

cancer cells by causing damage to proteins, DNA, and lipids. Here, we found that paroxetine treatment for 24 hours significantly increased the ROS level in AGS cells, but not in MKN-45 cells (**Figure 6A**). In general, most ROS is produced in mitochondria. We observed that paroxetine treatment of AGS cells increased the levels of ROS (**Figure 6B** and **6C**) and decreased the MMP (**Figure 6D-F**), indicating that this treatment might induce mitochondrial damage and consequently increase ROS production in AGS cells, but not in MKN-45 cells (**Figure 6G**).

To further decipher the role of ROS in paroxetine-mediated apoptosis and DNA damage, AGS cells were treated with paroxetine for 42 hours and co-treated with the GSH precursor, NAC (N-acetylcysteine, to prevent ROS generation) for 6 hours, and apoptosis- and DNA damage-related proteins were determined. NAC did not interfere with the ability of paroxetine to induce cleaved caspase 3, PARP (**Figure 7A**), or the assessed DNA damage markers and DNA repair proteins (γ-H2AX, phospho-Chk1, Rad51, HR23B, and ERCC1) (**Figure 7B**). Based on these findings, we speculate that ROS generation might not play a critical role in paroxetine-mediated DNA damage, at least in our experimental condition. Our further results suggested that ROS also might not significantly contribute to paroxetine-mediated autophagy (**Figure 7C**). However, the paroxetine-induced JNK signaling was reversed by NAC (**Figure 7D**), suggesting that ROS generation might act specifically in paroxetine-induced JNK signaling. Of note, whereas induced JNK activity increased apoptosis and DNA damage but decreased autophagy in paroxetine-treated AGS cells, activated ERK decreased apoptosis and enhanced autophagy (**Figure 7E**). This suggests that JNK and ERK may play opposing roles in paroxetine-mediated DNA damage, apoptosis, and autophagy in AGS cells.

Paroxetine acts as a chemosensitizer to synergistically enhance the effects of conventional anticancer drugs on MKN-45 cells

Emerging preclinical evidence indicates that combination therapies can promote anticancer effcacy without elevating toxicity. Since SSRIs have been reported to act as chemosensitizers to enhance chemotherapeutic effects [31], we hypothesized that paroxetine might act as a chemosensitizer for current anticancer drugs in MKN-45 cells. We used the CompuSyn software to determine the combination index (CI) from cytotoxicity results obtained using different concentrations of paroxetine alone or in combination with various chemotherapeutics. The CI showed that there was a potent synergy of cytotoxicity for paroxetine in combination with 5-fluorouracil (5-FU) or cisplatin at all tested combinations in MKN-45 cells (**Figure 8A** and **8B**). Likewise, a synergistic effect was evident for seven of the nine combination with doxorubicin, and six of the nine combinations with docetaxel (**Figure 8C** and **8D**). For further experiments, we chose the combinations of 10 μM paroxetine with 5-FU, cisplatin, docetaxel, and doxorubicin, which showed high synergistic effects. We next sought to clarify the synergistic effects of paroxetine in combination with these chemotherapeutic drugs. We found that co-treatment with 10 μM paroxetine increased the susceptibility of MKN-45 cells to the four chemotherapeutic drugs, as shown by increases in the sub-G1 fraction (**Figure 9A** and **9B**), activated caspase 3, cleaved PARP, and Bax (**Figure 9C**).

Collectively, our data reveal that a low nucleoside supply and insufficient DNA repair ability may play key roles in the paroxetine-induced DNA damage and cytotoxicity of AGS cells. We also show that combining paroxetine with conventional chemotherapeutic drugs could help sensitize patients with advanced gastric cancer to reduce cytotoxicity and overcome drug resistances induced by conventional chemotherapeutics, such as 5-FU, cisplatin, docetaxel, or doxorubicin. Future work is warranted to assess the potential synergistic effects of paroxetine and various chemotherapeutics on different cancers.

Discussion

In addition to its antidepressant activity, paroxetine has been shown to exert potent anticancer properties by inducing cell death and/or arresting the proliferation of cancer cells, both in vitro and in vivo. However, the mechanism underlying these effects remained unknown, and little information was available on the genotoxic effects of paroxetine. Here, we sought to gain a thorough understanding of the molecular mechanisms underlying the anticancer effects of paroxetine and its potential to treat gastric cancers. We reveal that AGS cells are susceptible to paroxetine in the micromolar range, whereas MKN-45 cells are less sensitive. Mechanistically, paroxetine inhibits cell proliferation in AGS cells via inhibiting the ex-

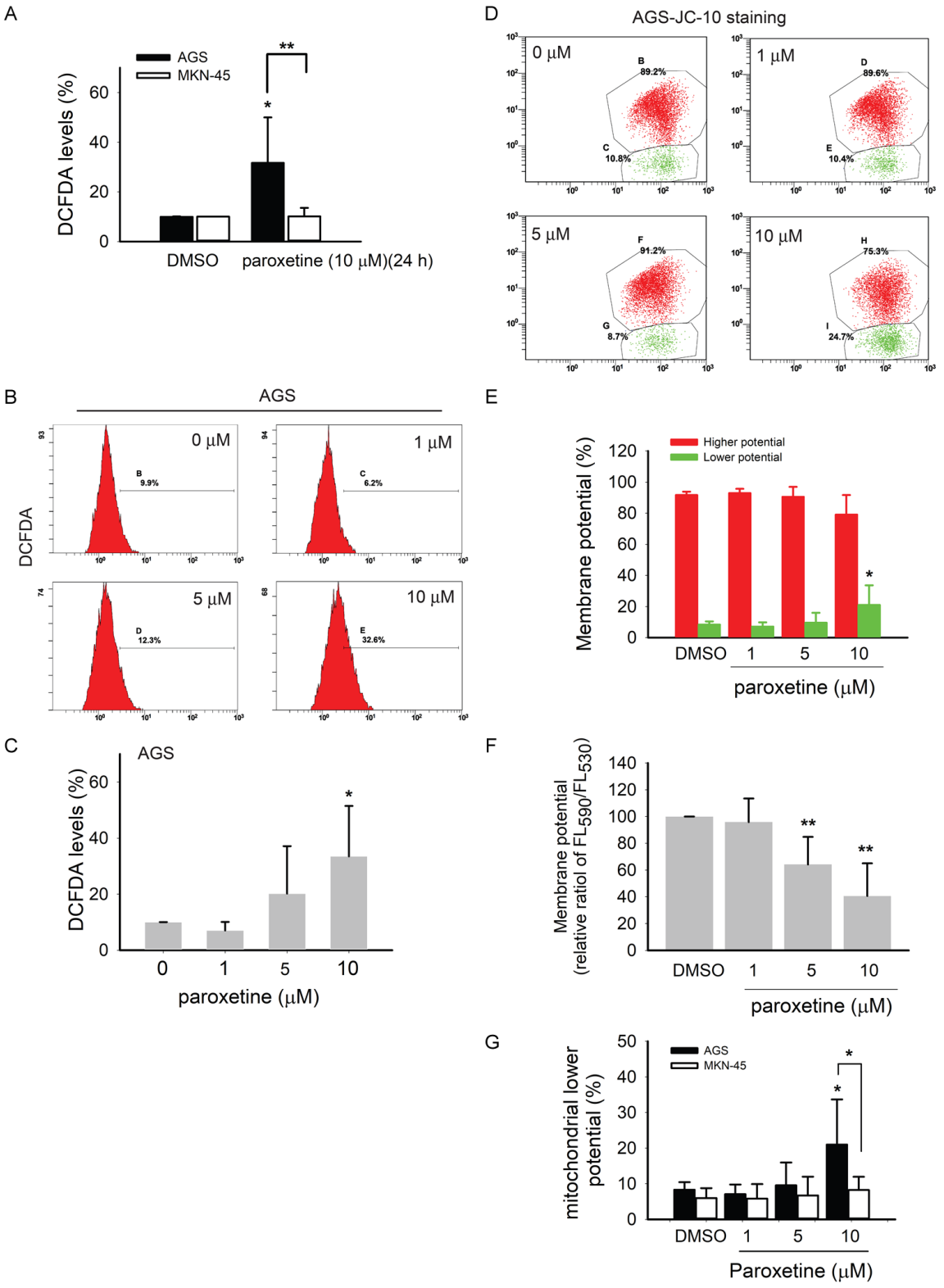

Figure 6. ROS generation was induced by paroxetine. (A) Cells were treated with 10 μM paroxetine for 24 hours and the levels of ROS were measured by DCFDA staining followed by flow cytometry. (B, C) AGS cells were exposed to different doses of paroxetine for 24 hours and the levels of ROS were measured. (D-G) Cells were co-treated with 10 μM paroxetine and 10 μM JC-10 reagent for 24 hours, and then subjected to flow cytometry analysis. Changes in the MMP of the cells by paroxetine were analyzed using flow cytometry (D) and quantified (E-G). JC-10 monomer (lower potential, FL530) and JC-10 aggregate (higher potential, FL590) are represented in green and red, respectively. Data are representative of three to five independent experiments.

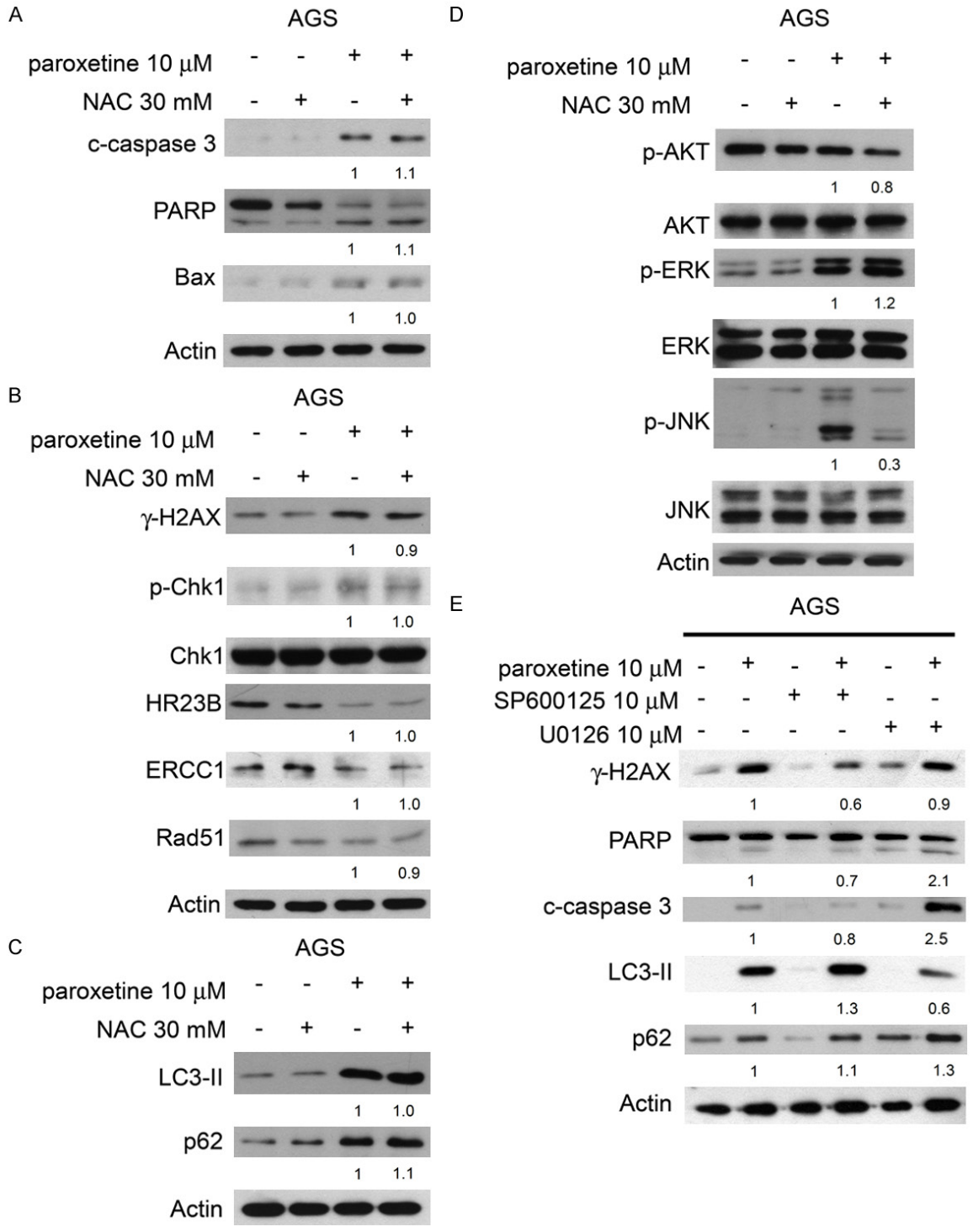

Figure 7. ROS does not contribute to paroxetine-induced DNA damage, apoptosis, or autophagy. AGS was treated with 10 μM paroxetine for 42 hours and then co-treated with NAC for another 6 hours. The protein levels of apoptosis (A), DNA damage and repair (B), autophagy (C), and signaling molecules (D) were measured by Western blot assays. (E) Cells were pre-exposed to U0126 and SP600125 for 1 hour and then co-treated with 10 μM paroxetine for another 24 hours. The protein levels of γ-H2AX, apoptosis, and autophagy markers were then determined by Western blot assays. Data are representative of three to five independent experiments.

pression of DNA repair proteins and increasing DNA damage, leading to the activation of apoptotic cell death. Conversely, paroxetine did not induce significant DNA damage or apoptosis in MKN-45 cells. Paroxetine treatment of AGS cells decreases the mRNA and protein levels of

A

paroxetine (μM)	5-FU (μM)	effect	CI
1	5	0.43	0.73262
1	10	0.6	0.78572
1	20	0.72	0.96882
5	5	0.49	0.64373
5	10	0.64	0.70236
5	20	0.75	0.85984
10	5	0.45	0.82486
10	10	0.65	0.70725
10	20	0.74	0.92096

B

paroxetine (μM)	cisplatin (μg/ml)	effect	CI
1	1	0.57	0.45732
1	2.5	0.67	0.79250
1	5	0.79	0.94676
5	1	0.66	0.35697
5	2.5	0.7	0.72578
5	5	0.81	0.86353
10	1	0.71	0.31631
10	2.5	0.73	0.66242
10	5	0.82	0.82882

C

paroxetine (μM)	docetaxel (nM)	effect	CI
1	1	0.44	0.82038
1	2	0.62	0.70115
1	4	0.58	1.68975
5	1	0.53	0.58616
5	2	0.67	0.56842
5	4	0.63	1.35625
10	1	0.67	0.32751
10	2	0.73	0.43006
10	4	0.67	1.13683

D

paroxetine (μM)	doxorubicin (nM)	effect	CI
1	50	0.54	0.56180
1	100	0.66	0.73713
1	200	0.74	1.07372
5	50	0.64	0.42622
5	100	0.71	0.62828
5	200	0.75	1.04342
10	50	0.74	0.30702
10	100	0.75	0.54970
10	200	0.81	0.79436

Figure 8. The synergistic effects of Paroxetine combination on cell viability in MKN-45 cells. A-D. MKN45 cells were treated with 10 μM paroxetine in combination with each of the listed anticancer drugs for 72 hours, and cell viability was assessed using the CCK-8. The combined effect of drug interactions was evaluated using a combination index (CI)-isobologram equation method, as described in the Materials and Methods. Data are representative of three to four independent experiments.

Rad51, HR23B, and ERCC1. Taken together, these findings lead us to propose a model in which increased DNA damage and attenuated DNA repair activity contribute to paroxetine-mediated cytotoxicity in AGS cells (**Figure 10**). The response of Rad51, HR23B, and ERCC1 levels in cancer cells under paroxetine treatment may be useful information when seeking to stratify patients for paroxetine treatment. Our data also suggest that due to genetic differences between MKN-45 and AGS cells, paroxetine may act as a sensitizer for chemotherapy in the former but as an independent chemotherapeutic drug in the latter. Synergistic combination therapy with paroxetine could enable effective treatment with lower doses of current chemotherapeutics and help avoid or overcome resistance. Going forward, we plan to use an NGS approach to investigate whether paroxetine systematically regulates other DNA repair-related proteins in AGS cells. We will also further examine how paroxetine interferes with DNA repair activities (e.g., homologous recombination repair and/or nucleotide excision repair) by downregulating the expression of Rad51/HR23B.

We previously identified potential POU3F2 binding sites in the promoter regions of the genes encoding Rad51, HR23B, and ERCC1 [32]. Our preliminary data show the mRNA level of POU3F2 was decreased in paroxetine-treated AGS cells (Supplemental Figure 2A). We speculate that paroxetine could negatively reg-

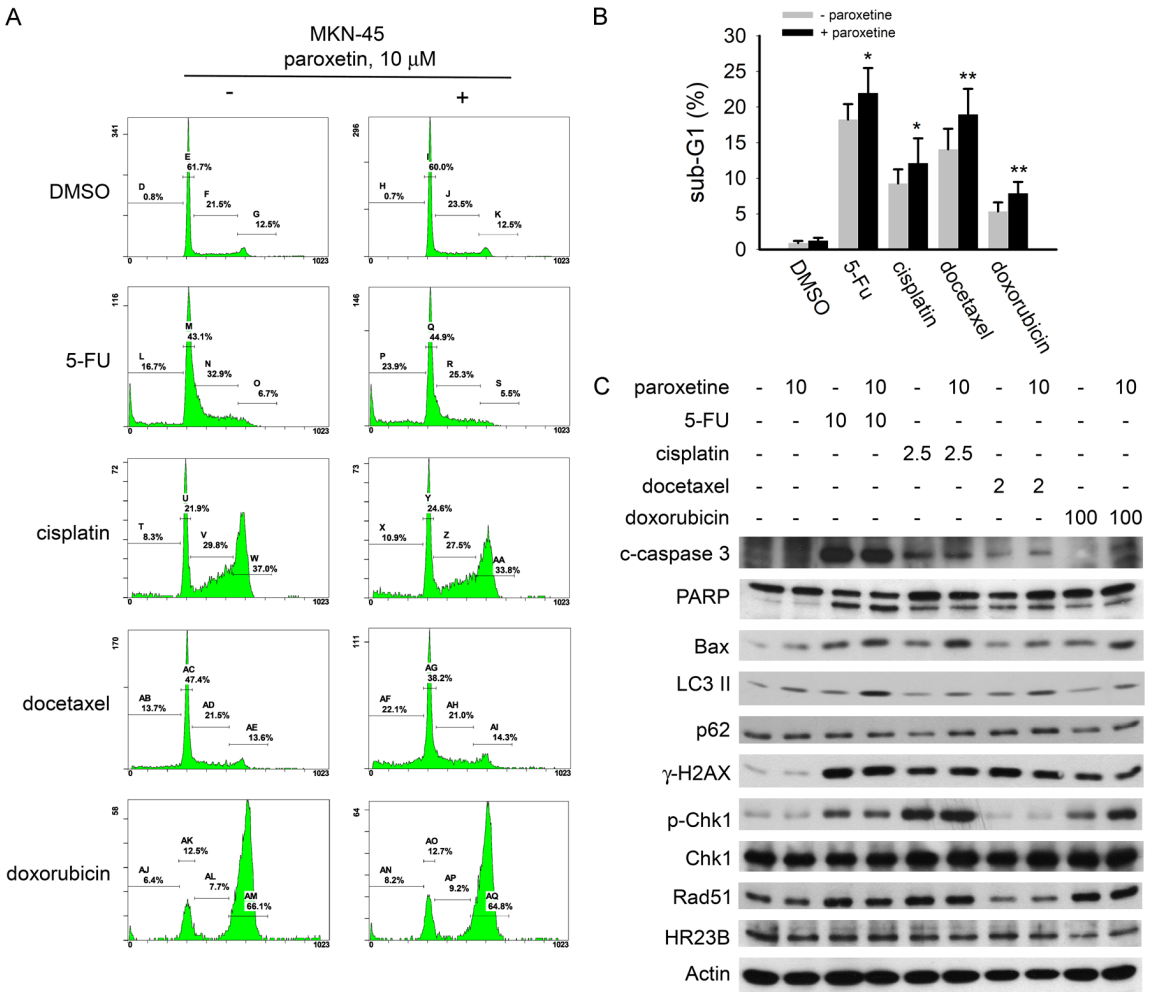

Figure 9. Paroxetine enhances anticancer agents-induced cytotoxicity in MKN-45. A, B. MKN-45 cells were co-treated with 10 μM paroxetine and 10 μM 5-FU, 2.5 μg/ml cisplatin, 2 nM docetaxel, and 100 nM doxorubicin for 72 hours, and the levels of sub-G1 were assayed by flow cytometry. C. MKN-45 cells were co-treated with 10 μM paroxetine and each of the listed anticancer drugs for 72 hours, and the corresponding levels of specific proteins associated with (related to) apoptosis, autophagy, and DNA damage responses were analyzed by Western blotting analysis. Data are representative of three to four independent experiments.

ulate POU3F2 expression, leading to the observed downregulations of Rad51, HR23B, and ERCC1. However, the detailed molecular mechanism by which paroxetine downregulates POU3F2 expression through transcriptional regulation warrants further investigation. We also found that the protein level of POU3F2 was remarkably decreased by paroxetine in AGS cells but not in MKN-45 cells (Supplemental Figure 2B), and note that the endogenous level of POU3F2 is lower in MKN-45 cells than in AGS cells. POU3F2 has attracting growing attention not only for its roles in neuronal development and reprogramming, but also because of its increasingly recognized role in a range of cancers [33, 34]. We also suggest that the ability of paroxetine to attenuate POU3F2 expression and function leads to the downregulations of Rad51, HR23B, and ERCC1, and thereby reveal a novel mechanism underlying the anticancer effects of paroxetine.

Although numerous studies have shown that SSRI class drugs exert cytotoxic effects on various cancer cells, the possible targets for these anticancer effects remained unknown. Paroxetine has been suggested to affect various signaling pathways via multiple mechanisms that differ in their dependence on 5-HT2/7 receptors [35]. The antiproliferative activity of paroxetine was thought to be independent of the serotonergic pathway, since acetylation of par-

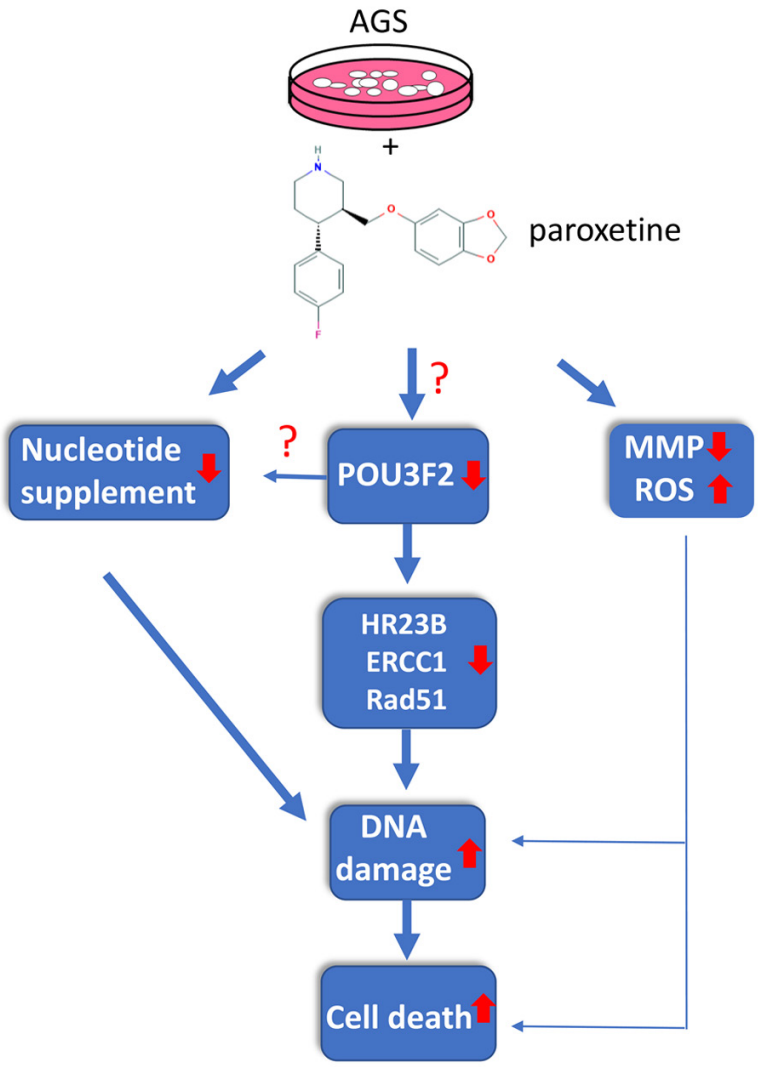

Figure 10. Schematic representation of paroxetine inducing DNA damage and cytotoxicity might be via shortage of nucleotides and DNA repair proteins in AGS. Our present results also suggest that paroxetine-enhanced ROS might contribute a miner effect on paroxetine-mediated DNA damage and cytotoxicity.

oxetine was found to abrogate its ability to inhibit 5-HT uptake without impairing its cytotoxic activity [8, 36]. Paroxetine was reported to modestly inhibit G protein-coupled receptor kinase 2 (GRK2), with an IC50 of 1.4 μM [19]. Jang et al. proposed that paroxetine might act through the inhibition of two major receptor tyrosine kinases, MET and ERBB3, leading to suppression of downstream survival signaling and activation of JNK-mediated apoptosis [16]. Using crystallographic analysis, Thal et al. found that GRK2 is a direct target for paroxetine and identified binding between paroxetine and the active site of GRK2 [19]. Paroxetine was suggested to affect cellular energy metabolism by directly binding and activating phosphofructokinase (PFK) in mouse brain [20]. Interestingly, using an inverse in silicoin vitro fishing strategy and kinase assay, Zhou et al. demonstrated that paroxetine effectively inhibits c-Src family kinases (e.g. ABL, SRC, KIT, MET, and FYN) in vitro [21]. We believe that identification of other novel targets will facilitate efforts to decipher the mechanisms underlying the anticancer actions of paroxetine. Here, we found that Rad51, HR23B, and ERCC1 are downregulated by paroxetine, and that their encoding genes might be downstream targets of POU3F2. Interestingly, Herbert et al. reported that POU3F2 associates with DNA damage response proteins at DNA damage sites to reprogram DNA damage repair, and that this contributes to the generation of melanoma with a high mutational burden [37]. Here, we provide new insights into the role of POU3F2 in DNA repair protein expression in the presence of paroxetine. However, additional work is needed to further investigate the transcriptional regulatory role of POU3F2 on downregulating the expression of Rad51, HR23B, and ERCC1 in paroxetine-treated AGS cells.

Our study uncovered a unique anticancer role for paroxetine and clearly showed that the inhibition of cell viability by paroxetine was much higher in AGS cells than in MKN-45 cells, suggesting that there may be a genetic basis for the difference in sensitivity to this agent. When exposed to the same concentration of paroxetine for 48 hours, the inhibition of cell viability in AGS cells was more than 4-fold that seen in MKN-45 cells. We initially hypothesized that the higher susceptibility of AGS cells to parox-

etine might arise from the ability of paroxetine to downregulate the POU3F2-Rad51/HR23B axis more effectively in AGS cells than in MKN-45 cells. Our results suggest that paroxetine might directly modulate cell biological processes, such as gene transcription or nucleoside/nucleotide metabolism. Meanwhile, we cannot exclude the possibility that paroxetine might directly attack and damage DNA. Given that the nucleoside transporters are responsible for the transmembrane influx of hydrophilic nucleosides, we are planning future studies aimed at examining the effect of paroxetine on the expression or function of nucleoside transporters. To our knowledge, this is the first report to indicate that paroxetine has a genotoxic effect in human cells, although other SSRIs, such as fluoxetine and citalopram, have been reported to enhance genotoxicity in mice and non-mammalian models [38, 39]. The relevant mechanisms and molecular targets for paroxetine-downregulated gene expression in vivo are still mystery. Although ROS may induce genotoxicity, additional work is needed to assess whether paroxetine interacts directly with genetic material, or whether it first requires metabolic transformation.

Drug biotransformation depends on two phases: phase I (oxidation), which covers the redox or hydrolytic reactions that convert lipophilic drugs into more polar metabolites (e.g., alcohols, phenols and carboxylic acids); and phase II (conjugation), which forms products that are readily excreted in urine, such as glucuronides and sulfates. Most phase I reactions are catalyzed by CYP450, which is localized mostly in the liver. It is well-known that drug interactions may compromise or enhance the effectiveness of anticancer agents. Tamoxifen, which is a selective modulator of estrogen receptors, is converted to its active metabolite, endoxifen, by the highly polymorphic and well-studied CYP450 family member, CYP2D6. Several studies have shown that drugs that inhibit CYP2D6 can reduce the clinical benefit of tamoxifen. Some SSRIs have been shown to inhibit CYP-2D6 to varying degrees; among them, paroxetine was found to inactivate various CYP450 family enzymes, including CYP2D6 [18]. Breast cancer patients taking some SSRIs (e.g., paroxetine) may have lower responses to tamoxifen therapy, arising from reduced formation of endoxifen. There is some debate around this effect, however: Kelly et al. found an association between paroxetine and increased risk of death from breast cancer [13], while Haque et al. did not observe an increased risk of subsequent breast cancer in women who concurrently used tamoxifen and antidepressants, including paroxetine [40] and Donneyong et al. reported that concomitant use of tamoxifen and potent CYP2D6-inhibiting SSRIs was not associated with an increased risk of death from breast cancer versus the co-use of other SSRIs [41]. Thus, it remains unclear whether there is a clinically significant interaction between SSRIs and tamoxifen. There is no evidence to date that the metabolism of 5-FU, cisplatin, or doxorubicin involve the CYP450 system. Docetaxel is metabolized and inactivated by CYP3A4, suggesting that the use of a CYP3A4 inhibitor with docetaxel may benefit the treatment of cancer [42]. Our present study revealed that the levels of paroxetine metabolites were not different between AGS and MKN-45 cells, indicating that a metabolic mechanism might not cause the difference in paroxetine susceptibility between these cell lines.

Our results indicate that concomitant use of paroxetine and 5-FU, cisplatin, docetaxel, or doxorubicin can yield synergistically enhanced cytotoxic effects in MKN-45 cells. Since these four anticancer drugs can induce ROS generation, DNA damage, the formation of DNA adducts, and the inhibition of transcription and replication, future work is needed to assess whether paroxetine is sufficient to alter other biological pathways.

Acknowledgements

This work was supported by a grant from the Ministry of Health and Welfare, Feng Yuan Hospital Research Project 108-002; and the Research Project of Ministry of Health and Welfare (grant number 11014), Taiwan.

Disclosure of conflict of interest

None.

Address correspondence to: Yi-Mei J Lin and Show-Mei Chuang, Institute of Biomedical Sciences, National Chung Hsing University, 145 Xingda Road, Taichung 402, Taiwan. Tel: 886-4-22840896; Fax: 886-4-22853469; E-mail: ymjlin@nchu.edu.tw (YMJL); smchuang@dragon.nchu.edu.tw (SMC)

References

[1] Calcabrini C, Maffei F, Turrini E and Fimognari C. Sulforaphane potentiates anticancer effects of doxorubicin and cisplatin and mitigates their toxic effects. Front Pharmacol 2020; 11: 567.

[2] Li H, Krstin S, Wang S and Wink M. Capsaicin and piperine can overcome multidrug resistance in cancer cells to doxorubicin. Molecules 2018; 23: 557.

[3] Tan BL and Norhaizan ME. Curcumin combination chemotherapy: the implication and efficacy in cancer. Molecules 2019; 24: 2527.

[4] Vendrely V, Peuchant E, Buscail E, Moranvillier I, Rousseau B, Bedel A, Brillac A, de Verneuil H, Moreau-Gaudry F and Dabernat S. Resveratrol and capsaicin used together as food complements reduce tumor growth and rescue full efficiency of low dose gemcitabine in a pancreatic cancer model. Cancer Lett 2017; 390: 91-102.

[5] Chou CT, He S and Jan CR. Paroxetine-induced apoptosis in human osteosarcoma cells: activation of p38 MAP kinase and caspase-3 pathways without involvement of [Ca2+]i elevation. Toxicol Appl Pharmacol 2007; 218: 265-273.

[6] Gil-Ad I, Zolokov A, Lomnitski L, Taler M, Bar M, Luria D, Ram E and Weizman A. Evaluation of the potential anti-cancer activity of the antidepressant sertraline in human colon cancer cell lines and in colorectal cancer-xenografted mice. Int J Oncol 2008; 33: 277-286.

[7] Kuwahara J, Yamada T, Egashira N, Ueda M, Zukeyama N, Ushio S and Masuda S. Comparison of the anti-tumor effects of selective serotonin reuptake inhibitors as well as serotonin and norepinephrine reuptake inhibitors in human hepatocellular carcinoma cells. Biol Pharm Bull 2015; 38: 1410-1414.

[8] Rosetti M, Frasnelli M, Tesei A, Zoli W and Conti M. Cytotoxicity of different selective serotonin reuptake inhibitors (SSRIs) against cancer cells. J Exp Ther Oncol 2006; 6: 23-29.

[9] Serafeim A, Holder MJ, Grafton G, Chamba A, Drayson MT, Luong QT, Bunce CM, Gregory CD, Barnes NM and Gordon J. Selective serotonin reuptake inhibitors directly signal for apoptosis in biopsy-like burkitt lymphoma cells. Blood 2003; 101: 3212-3219.

[10] Xu W, Tamim H, Shapiro S, Stang MR and Collet JP. Use of antidepressants and risk of colorectal cancer: a nested case-control study. Lancet Oncol 2006; 7: 301-308.

[11] Morch LS, Dehlendorff C, Baandrup L, Friis S and Kjaer SK. Use of antidepressants and risk of epithelial ovarian cancer. Int J Cancer 2017; 141: 2197-2203.

[12] Chubak J, Bowles EJ, Yu O, Buist DS, Fujii M and Boudreau DM. Breast cancer recurrence in relation to antidepressant use. Cancer Causes Control 2016; 27: 125-136.

[13] Kelly CM, Juurlink DN, Gomes T, Duong-Hua M, Pritchard KI, Austin PC and Paszat LF. Selective serotonin reuptake inhibitors and breast cancer mortality in women receiving tamoxifen: a population based cohort study. BMJ 2010; 340: c693.

[14] Levkovitz Y, Gil-Ad I, Zeldich E, Dayag M and Weizman A. Differential induction of apoptosis by antidepressants in glioma and neuroblastoma cell lines: evidence for p-c-Jun, cytochrome c, and caspase-3 involvement. J Mol Neurosci 2005; 27: 29-42.

[15] Cho YW, Kim EJ, Nyiramana MM, Shin EJ, Jin H, Ryu JH, Kang KR, Lee GW, Kim HJ, Han J and Kang D. Paroxetine induces apoptosis of human breast cancer MCF-7 cells through Ca(2+)- and p38 MAP kinase-dependent ROS generation. Cancers (Basel) 2019; 11: 64.

[16] Jang WJ, Jung SK, Vo TTL and Jeong CH. Anticancer activity of paroxetine in human colon cancer cells: involvement of MET and ERBB3. J Cell Mol Med 2019; 23: 1106-1115.

[17] Wang K, Gong Q, Zhan Y, Chen B, Yin T, Lu Y, Zhang Y, Wang H, Ke J, Du B, Liu X and Xiao J. Blockage of autophagic flux and induction of mitochondria fragmentation by paroxetine hydrochloride in lung cancer cells promotes apoptosis via the ROS-MAPK pathway. Front Cell Dev Biol 2020; 7: 397.

[18] Desmarais JE and Looper KJ. Interactions between tamoxifen and antidepressants via cytochrome P450 2D6. J Clin Psychiatry 2009; 70: 1688-1697.

[19] Thal DM, Homan KT, Chen J, Wu EK, Hinkle PM, Huang ZM, Chuprun JK, Song J, Gao E, Cheung JY, Sklar LA, Koch WJ and Tesmer JJ. Paroxetine is a direct inhibitor of g protein-coupled receptor kinase 2 and increases myocardial contractility. ACS Chem Biol 2012; 7: 1830-1839.

[20] Park DI, Novak B, Yan Y, Kaya ME and Turck CW. Paroxetine binding and activation of phosphofructokinase implicates energy metabolism in antidepressant mode of action. J Psychiatr Res 2020; 129: 8-14.

[21] Zhou W, Yang H and Wang H. Inverse in silico-in vitro fishing of unexpected paroxetine kinase targets from tumor druggable kinome. J Mol Model 2020; 26: 197.

[22] Liang RY, Liu BH, Huang CJ, Lin KT, Ko CC, Huang LL, Hsu B, Wu CY and Chuang SM. MEK2 is a critical modulating mechanism to down-regulate GCIP stability and function in cancer cells. FASEB J 2020; 34: 1958-1969.

[23] Lin RJ, Wu IJ, Hong JY, Liu BH, Liang RY, Yuan TM and Chuang SM. Capsaicin-induced TRIB3 upregulation promotes apoptosis in cancer

cells. Cancer Manag Res 2018; 10: 4237-4248.
[24] Nabekura T, Kamiyama S and Kitagawa S. Effects of dietary chemopreventive phytochemicals on P-glycoprotein function. Biochem Biophys Res Commun 2005; 327: 866-870.
[25] Takatsuka R, Ito S, Iwai S and Kuraoka I. An assay to detect DNA-damaging agents that induce nucleotide excision-repairable DNA lesions in living human cells. Mutat Res Genet Toxicol Environ Mutagen 2017; 820: 1-7.
[26] Chou TC. Theoretical basis, experimental design, and computerized simulation of synergism and antagonism in drug combination studies. Pharmacol Rev 2006; 58: 621-681.
[27] Chou TC. Drug combination studies and their synergy quantification using the Chou-Talalay method. Cancer Res 2010; 70: 440-446.
[28] Bester AC, Roniger M, Oren YS, Im MM, Sarni D, Chaoat M, Bensimon A, Zamir G, Shewach DS and Kerem B. Nucleotide deficiency promotes genomic instability in early stages of cancer development. Cell 2011; 145: 435-446.
[29] Anglana M, Apiou F, Bensimon A and Debatisse M. Dynamics of DNA replication in mammalian somatic cells: nucleotide pool modulates origin choice and interorigin spacing. Cell 2003; 114: 385-394.
[30] Segura M, Roura L, de la Torre R and Joglar J. Synthesis of the major metabolites of paroxetine. Bioorg Chem 2003; 31: 248-258.
[31] Amit BH, Gil-Ad I, Taler M, Bar M, Zolokov A and Weizman A. Proapoptotic and chemosensitizing effects of selective serotonin reuptake inhibitors on T cell lymphoma/leukemia (Jurkat) in vitro. Eur Neuropsychopharmacol 2009; 19: 726-734.
[32] Lin YJ, Hsin IL, Sun HS, Lin S, Lai YL, Chen HY, Chen TY, Chen YP, Shen YT and Wu HM. NTF3 is a novel target gene of the transcription factor POU3F2 and is required for neuronal differentiation. Mol Neurobiol 2018; 55: 8403-8413.
[33] Cook AL and Sturm RA. POU domain transcription factors: BRN2 as a regulator of melanocytic growth and tumourigenesis. Pigment Cell Melanoma Res 2008; 21: 611-626.
[34] Purkayastha BP and Roy JK. Cancer cell metabolism and developmental homeodomain/POU domain transcription factors: a connecting link. Cancer Lett 2015; 356: 315-319.
[35] Durairaj H, Steury MD and Parameswaran N. Paroxetine differentially modulates LPS-induced TNFalpha and IL-6 production in mouse macrophages. Int Immunopharmacol 2015; 25: 485-492.
[36] Schuster C, Fernbach N, Rix U, Superti-Furga G, Holy M, Freissmuth M, Sitte HH and Sexl V. Selective serotonin reuptake inhibitors--a new modality for the treatment of lymphoma/leukaemia? Biochem Pharmacol 2007; 74: 1424-1435.
[37] Herbert K, Binet R, Lambert JP, Louphrasitthiphol P, Kalkavan H, Sesma-Sanz L, Robles-Espinoza CD, Sarkar S, Suer E, Andrews S, Chauhan J, Roberts ND, Middleton MR, Gingras AC, Masson JY, Larue L, Falletta P and Goding CR. BRN2 suppresses apoptosis, reprograms DNA damage repair, and is associated with a high somatic mutation burden in melanoma. Genes Dev 2019; 33: 310-332.
[38] Gurbuzel M, Oral E, Kizilet H, Halici Z and Gulec M. Genotoxic evaluation of selective serotonin-reuptake inhibitors by use of the somatic mutation and recombination test in Drosophila melanogaster. Mutat Res 2012; 748: 17-20.
[39] Alzahrani HA. Sister chromatid exchanges and sperm abnormalities produced by antidepressant drug fluoxetine in mouse treated in vivo. Eur Rev Med Pharmacol Sci 2012; 16: 2154-2161.
[40] Haque R, Shi J, Schottinger JE, Ahmed SA, Cheetham TC, Chung J, Avila C, Kleinman K, Habel LA, Fletcher SW and Kwan ML. Tamoxifen and antidepressant drug interaction in a cohort of 16,887 breast cancer survivors. J Natl Cancer Inst 2016; 108: djv337.
[41] Donneyong MM, Bykov K, Bosco-Levy P, Dong YH, Levin R and Gagne JJ. Risk of mortality with concomitant use of tamoxifen and selective serotonin reuptake inhibitors: multi-database cohort study. BMJ 2016; 354: i5014.
[42] Miguel C and Albuquerque E. Drug interaction in psycho-oncology: antidepressants and antineoplastics. Pharmacology 2011; 88: 333-339.

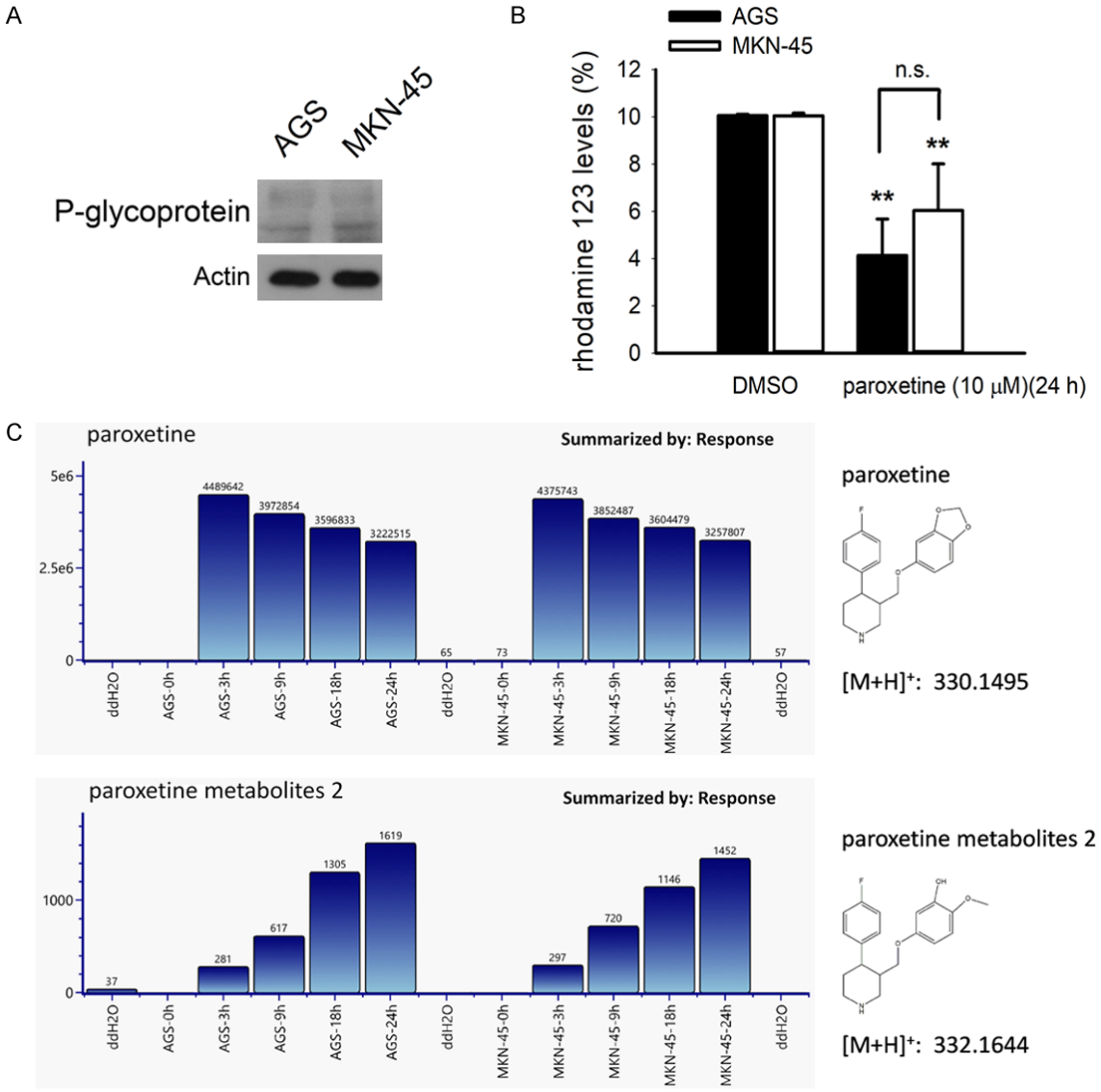

Supplemental Figure 1. (A) Cells were exposed to 10 μM paroxetine, and then the protein levels and xenobiotic exclusion ability of P-glycoprotein were determined by Western blot (A) and flow cytometry analysis (B). (C) Cells were exposed to 10 μM paroxetine and the cell cultured medium was collected to determine the metabolites of paroxetine using LC-MS/MS. Metabolite 3 cannot be detected.

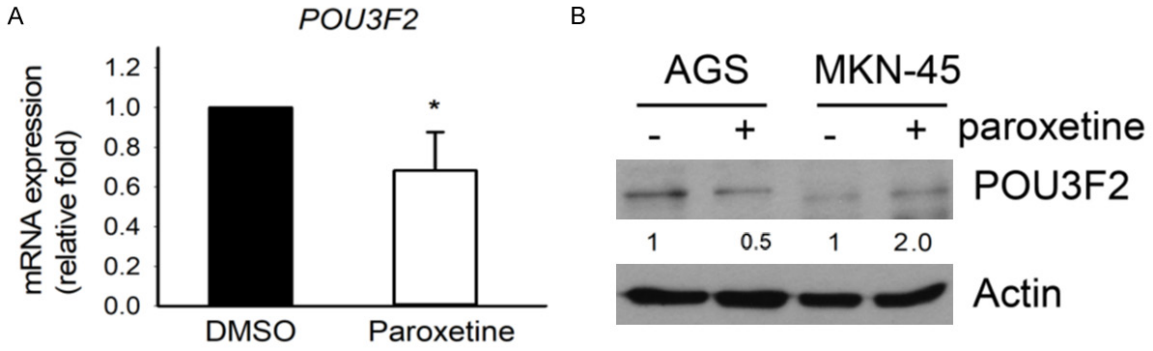

Supplemental Figure 2. A. After 24-hour treatment of 10 μM paroxetine, the mRNA levels of POU3F2 were determined by qRT-PCR. B. After 48-hour treatment of 10 μM paroxetine, the protein levels of POU3F2 were determined by Western blot assays.